Development 140, 1034-1044 (2013) doi:10.1242/dev.085225

Foxc1 controls the growth of the murine frontal bone rudiment by direct regulation of a Bmp response threshold of *Msx2*

Jingjing Sun, Mamoru Ishii, Man-Chun Ting and Robert Maxson*

SUMMARY

The mammalian skull vault consists of several intricately patterned bones that grow in close coordination. The growth of these bones depends on the precise regulation of the migration and differentiation of osteogenic cells from undifferentiated precursor cells located above the eye. Here, we demonstrate a role for Foxc1 in modulating the influence of Bmp signaling on the expression of *Msx2* and the specification of these cells. Inactivation of *Foxc1* results in a dramatic reduction in skull vault growth and causes an expansion of *Msx2* expression and Bmp signaling into the area occupied by undifferentiated precursor cells. Foxc1 interacts directly with a Bmp responsive element in an enhancer upstream of *Msx2*, and acts to reduce the occupancy of P-Smad1/5/8. We propose that Foxc1 sets a threshold for the Bmp-dependent activation of *Msx2*, thus controlling the differentiation of osteogenic precursor cells and the rate and pattern of calvarial bone development.

KEY WORDS: Skull vault, Foxc1, Msx2, Bmp responsive element, Mouse

INTRODUCTION

Knowing how signaling molecules elicit transcriptional responses of target genes at specific thresholds is crucial for understanding cell specification during embryonic patterning. A key element of such mechanisms is the complement of transcription factors that respond to the signal and influence the expression of downstream genes (Gurdon et al., 1995; Gurdon and Bourillot, 2001). Although a number of these factors have been identified, how their transcription regulatory activity is translated into events at the level of cell specification and patterned growth is still incompletely understood. Here, we investigate the role of Foxc1 in modulating the influence of Bmp signaling on the expression of the Bmp effector *Msx2*, and the specification of osteogenic precursor cells in the developing skull vault.

The mammalian skull vault consists of a group of intricately patterned bones that develop in close coordination (Morriss-Kay and Wilkie, 2005; Chai and Maxson, 2006). These include the paired frontal and parietal bones. The frontal bones are derived from cranial neural crest and the parietal bones from head mesoderm. In the mouse embryo, skull vault precursor cell populations migrate into positions above the eye by E12.5. There they condense and begin to differentiate into the calvarial rudiments. From E13.5 into postnatal development, the paired frontal and parietal bone rudiments grow apically, coming into apposition at the midline at the frontal and sagittal sutures, and laterally at the coronal suture.

The morphogenetic mechanisms underlying the patterned growth of the calvarial bones are under active investigation. Proliferation of osteogenic cells within the rudiments contributes to growth (Ishii et al., 2003), as does the apical migration of osteogenic precursor cells. DiI labeling experiments show that a population of such migratory osteogenic precursor (MOP) cells is located outside (ectocranial to) the rudiments; cells from this population migrate apically, insert into the leading edge of the growing rudiment and differentiate into osteoblasts (Yoshida et al., 2008; Ting et al., 2009; Roybal et al., 2010).

Msx genes, effectors of Bmp signaling, are crucial for calvarial development (Satokata et al., 2000; Wilkie et al., 2000; Chai and Maxson, 2006). Msx genes are an ancient and highly conserved homeobox gene family with a variety of functions in vertebrate organogenesis (Satokata and Maas, 1994; Phippard et al., 1996; Bach et al., 2003; Chen et al., 2007). *Msx1* and *Msx2* are well known as downstream targets of the Bmp signaling pathway, and at the same time can regulate the expression of Bmp ligands (Bei and Maas, 1998). In $Msx2^{-/-}$ embryos, the growth of the calvarial rudiments is deficient, resulting in a large ossification defect in the frontal bone (Ishii et al., 2003). Humans with heterozygous loss of *MSX2* function are similarly affected (Wilkie et al., 2000). Combination *Msx1*/*2* mutants exhibit agenesis of the frontal and parietal bones (Han et al., 2007).

Msx2 is regulated by the Bmp pathway through an upstream Bmp responsive enhancer element (Brugger et al., 2004). This element, ~560 bp in length, contains a 52 bp fragment necessary for the Bmp responsiveness of an *Msx2* transgene in embryos and in cultured cells. This fragment contains an AT-rich central sequence flanked by Smad-binding sites. Both the AT-rich site and the Smad sites are required for Bmp responsiveness. The AT-rich region contains a partial Fox consensus site (Gao et al., 2003; Brugger et al., 2004; Benayoun et al., 2011), leading us to propose that Fox proteins function together with Smads to regulate the ability of *Msx2* to respond to Bmp signaling (Brugger et al., 2004). Here, we present genetic and molecular evidence that the Fox protein Foxc1 controls the Bmp responsiveness of *Msx2*.

Fox genes are involved in a variety of developmental processes during organogenesis, as well as in aspects of energy homeostasis and cancer (Hannenhalli and Kaestner, 2009; Benayoun et al., 2011). Both targeted ($Foxc1^{lacZ}$) and spontaneous ($Foxc1^{ch}$) *Foxc1*-null mice die perinatally with identical skeletal, ocular, genitourinary, cardiovascular and somitic defects, as well as hydrocephalus and cerebellar defects (Kume et al., 1998; Kume et

Department of Biochemistry and Molecular Biology, Norris Cancer Hospital, University of Southern California Keck School of Medicine, 1441 Eastlake Avenue, Los Angeles, CA 90089-9176, USA.

*Author for correspondence (maxson@usc.edu)

Accepted 18 December 2012

al., 2000; Kume et al., 2001; Seo and Kume, 2006). The most striking skeletal phenotype in *Foxc1* mutant mice is the lack of calvarial bones. This defect is not secondary to hydrocephalus (Rice et al., 2003). Recently, a new mouse model with a hypomorphic allele of *Foxc1* (*Foxc1*^{hith}) was found to have meningeal defects in association with frontal foramina and cortical dysplasia (Zarbalis et al., 2007). In humans, mutations in *FOXC1* are associated with Axenfeld-Rieger and Dandy Walker syndromes, both inherited as autosomal dominant traits. Individuals affected with Axenfeld-Rieger syndrome exhibit a spectrum of malformations, including dysgenesis of the anterior segment of the eye, tooth abnormalities, maxillary hypoplasia, hypertelorism and cardiac outflow tract defects (Tümer and Bach-Holm, 2009). Dandy-Walker syndrome, the most common human cerebellar malformation, is associated with deletions or duplications spanning the *FOXC1* gene (Aldinger et al., 2009).

We report here that Foxc1 controls the differentiation of osteogenic precursor cells that contribute to the frontal bone, and we present evidence that it does so by inhibiting the Bmp responsiveness of *Msx2* and the activity of the Bmp pathway in such cells. We show further that Foxc1 interacts directly with a Bmp-responsive element in the *Msx2* 560 bp upstream enhancer, and we confirm, by means of gain- and loss-of-function experiments in a newly developed cranial neural crest cell line (Ishii et al., 2012), that Foxc1 acts as a negative regulator of the Bmp responsiveness of *Msx2*. We show finally that Foxc1 acts to restrict the occupancy of P-Smad1/5/8 on the *Msx2* Bmp responsive element. We propose that the normal function of Foxc1 is to set a transcriptional threshold for the Bmp-dependent activation of *Msx2*, thus controlling the differentiation of osteogenic precursor cells and the initial phases of calvarial bone development.

MATERIALS AND METHODS

DNA constructs

Msx2 enhancer constructs *pBSK-560bpMsx2-hsplacZ*, *pBSK-52bpMsx2-hsplacZ*, *pBSK-52bpMsx2-mut-hsplacZ* and *pGL2-560bpMsx2-tk-luciferase* have been described previously (Brugger et al., 2004). The *Foxc1* expression vector *pcDNA3-mFoxc1* was a kind gift from Dr Tsutomu Kume (Northwestern University, Chicago, IL, USA).

Cell culture, co-transfections and luciferase assay

10T1/2 cells were propagated in DMEM with 10% FBS. O9-1 cells were maintained and differentiated into osteoblast as recently reported (Ishii et al., 2012). Lipofectamine 2000 (Life Technologies) was used to introduce *pcDNA3-mFoxc1* or siFoxc1 with *pGL2-560bpMsx2-tk-luc* into 10T1/2 and O9-1 cells. BMP2 (100 ng/ml) treatment and luciferase assay was performed as described previously (Brugger et al., 2004).

Mouse strains and genotyping

Heterozygous *Foxc1*$^{ch/+}$ (*ch: congenital hydrocephalus*) mice were purchased from Jackson Laboratory on the CHMU/Le background. *Msx2* mutant mice, originally obtained from Dr Richard Maas (Harvard University, Boston, MA, USA), were crossed into a C57BL/6 background (Ishii et al., 2003). *560bpMsx2-hsplacZ* transgenic mice have been described previously (Kwang et al., 2002). The *ch* allele of *Foxc1* was identified by PCR amplification followed by *Cac*8I digestion (Kume et al., 2000). The *Msx2* mutant allele and the *lacZ* transgene were identified by PCR (Satokata et al., 2000; Kwang et al., 2002).

Bead implantation

Preparation of the agarose beads and calvarial explant culture were performed as previously described (Rice et al., 2003; Brugger et al., 2004).

Histochemistry, immunostaining and *in situ* hybridization

lacZ, ALP histochemistry and immunofluorescent detection for P-Smad1/5/8 (Cell Signaling) have been described previously (Ishii et al., 2003; Ting et al., 2009). *Msx2* full-length cDNA was cloned into pBSKII(+) (Kwang et al., 2002). A cloned *Foxc1* cDNA was a kind gift from Dr David Rice (University of Helsinki, Finland). *Bmp2* and *Bmp4* full-length cDNAs were obtained from Dr Malcolm Snead (USC, Los Angeles, CA, USA). *Noggin* cDNA was a gift from Dr Richard Harland (UCLA, Berkeley, CA, USA). *Runx2* cDNA was obtained from Dr Gérard Karsenty (Columbia University Medical Center, NY, USA). Ribonucleotide probes were generated as described previously (Kwang et al., 2002). Fluorescent *in situ* hybridization followed by tyramide signal amplification (TSA PLUS, Perkin Elmer) was carried out as reported previously (Paratore et al., 1999; Ting et al., 2009).

To quantify ALP, *Msx2*, *Bmp4* and *Bmp2* expression, continuous sections from at least two wild-type and two mutant embryos were photographed and analyzed with Adobe Photoshop. We used the magic wand tool to select the region of interest and calculate the pixel numbers of selected area. Data show the average pixel count of ~10-15 pictures from one representative pair. For *Foxc1* and *Msx2* colocalization (Fig. 2G), yellow pixels were selected by color and counted from a total 16 sections of three pairs of control and mutant embryos. At least 10 pictures from three individuals of each genotype were analyzed to quantify the influence of *Msx2* dose on ectopic ALP (Fig. 4I) and P-Smad1/5/8 (Fig. 4N) expression.

RNAi and qRT-PCR

siRNAs targeting Foxc1 (Ambion, SMARTpool Dharmacon) were introduced into O9-1 or C3H10T1/2 cells by Lipofectamine 2000 (Life Technologies) according to the manufacturer's protocol. siGFP was used as control (supplementary material Table S1). Cells were collected ~24-48 hours after transfection and subjected to total RNA extraction with the RNeasy Mini Kit (Qiagen). First-strand cDNA was synthesized with the SuperScript III system (Life Technologies) for RT-PCR analysis. Relative expression levels were normalized to *Gapdh* mRNA. Primer sequences are given in supplementary material Table S1.

Chromatin immunoprecipitation (ChIP) assays

ChIP was performed as described previously (Ma et al., 2003; Brugger et al., 2004) with minor modifications. Cells were treated with 60 ng/ml BMP2 for 30 minutes prior to fixation. Anti-Foxc1 pull-down was achieved by two sessions of incubation: first with a goat anti-Foxc1 antibody (Abcam), then with a rabbit anti-goat IgG (Sigma-Aldrich). Rabbit IgG was used for mock immunoprecipitation (Sigma-Aldrich). qPCR was performed to amplify a 350 bp region of the endogenous *Msx2* enhancer. For transfected cells, DNA constructs or siRNA were introduced into cells 24 hours prior to BMP2 treatment. A 200 bp region of the *hsp68* mini-promoter immediately downstream of the 52 bp *Msx2* Bmpre in pBSK was amplified by qPCR. Each result is controlled by IgG, and is from a single experiment representative of three independent experiments. Primer sequences are given in supplementary material Table S1.

RESULTS

Foxc1 regulates the size of the frontal bone rudiment and the osteogenic differentiation of cultured cranial neural crest cells

We first examined the expression of an early osteoblast marker, alkaline phosphatase (ALP), in *Foxc1* mutant and control embryos at E12.5 (Fig. 1B-C′), E13.5 (Fig. 3D,D′,F,F′) and E14 (supplementary material Fig. S1A-B″). Consistent with previous findings (Ishii et al., 2003; Rice et al., 2003), ALP was expressed in control embryos in a group of cells that make up the frontal and parietal bone rudiments (Fig. 1B,C; Fig. 3D,F; supplementary material Fig. S1A,B). In *Foxc1*$^{ch/ch}$ mutants, apical growth did not progress beyond the primordium stage, and the rudiments mineralized by E15 with little or no further growth (supplementary material Fig. S1A″,B″) (Rice et al., 2003). These results are consistent with those of Rice and colleagues (Rice et al., 2003). In addition to this previously reported lack of apical growth, we found that the ALP-positive area expanded laterally toward the epidermis and ventrally towards the midline of the cranial base (arrows, Fig. 1C′). Quantitation of the ALP signal in

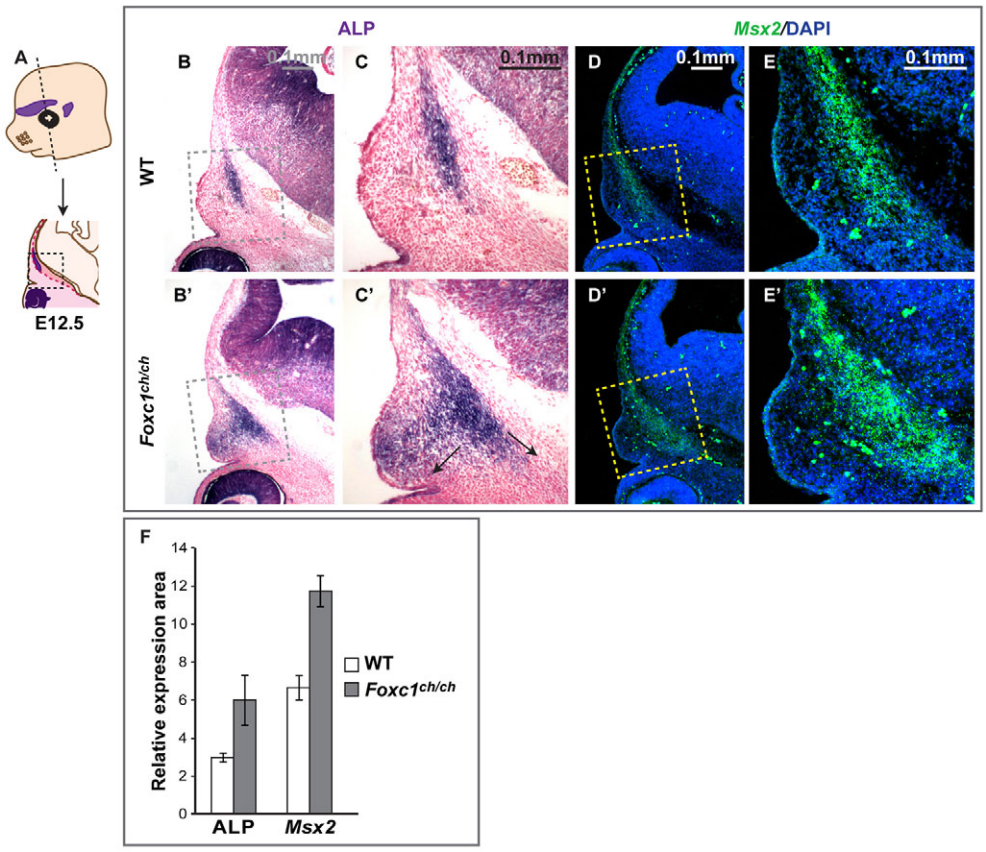

Fig. 1. Expansion of frontal bone osteogenic domain in the supraorbital ridge of *Foxc1* mutant embryos. (**A-E′**) Control (B-E) and *Foxc1*$^{ch/ch}$ mutant (B′-E′) embryos at E12.5 were sectioned in the indicated (coronal) plane (A) and stained for ALP to mark osteogenic cells (B-C′) or were subjected to *in situ* hybridization for *Msx2* (D-E′). Boxed areas are shown at higher magnification on the right. (**F**) Increased ALP-positive osteogenic progenitor domain and *Msx2* mRNA signal inside the boxed area in *Foxc1* mutant embryos (Student's *t*-test, $P<5.00\times10^{-5}$). Error bars indicate s.d.

serial sections through the supraorbital ridge confirmed this expansion ($P<5.00\times10^{-5}$, Fig. 1F). *Runx2*, also a pre-osteoblast marker, exhibited a similar expansion in *Foxc1* mutant embryos (supplementary material compare Fig. S1C with S1C″). *Foxc1* mutants have hydrocephalus, precluding analysis of skull vault growth and patterning in embryos after E15.

Lineage tracing with Wnt1-Cre/R26R (neural crest) and Mesp1-Cre/R26R (mesoderm) showed no major differences between *Foxc1* mutant and control embryos in the distribution of neural crest and mesoderm in the head region of E9.5 or E12.5 embryos (supplementary material Fig. S2). Thus, the lack of apical extension of the frontal and parietal bones is not likely to be caused by a failure of osteogenic precursor cells to migrate into position in the supraorbital ridge.

In situ hybridization revealed that *Msx2*, which is normally expressed in the osteogenic cells of the frontal and parietal rudiments (Fig. 1E), expanded laterally in *Foxc1*$^{ch/ch}$ mutants, coincident with the expansion in the ALP domain (arrows, Fig. 1C′; $P<1.00\times10^{-16}$, Fig. 1F). We used *Foxc1* and *Msx2* probes simultaneously to determine the relationship between the *Foxc1* expression domain and the expansion of *Msx2* expression (Fig. 2). Because the *Foxc1 ch* mutation is a single base change, the *Foxc1* transcript is detectible in sections of mutant embryos. At E11.5, *Msx2* was expressed broadly in cranial mesenchyme. *Foxc1* transcripts were detected mainly in the periocular mesenchyme and not in the mesenchyme where the frontal bone rudiment forms (data not shown). By E12.5, in control embryos, *Foxc1* was expressed in the meninges and in the cranial mesenchyme, overlapping partially with *Msx2* in the lateral region of the *Foxc1* domain (Fig. 2A,B). The number of cells expressing both *Foxc1* and *Msx2* transcripts (yellow pixels, Fig. 2G) increased in *Foxc1* mutants ($P<5.00\times10^{-4}$), consistent with an increase in *Msx2* transcripts in cells expressing the mutant *Foxc1* mRNA. *Msx2* expression also increased laterally outside the *Foxc1* domain (Fig. 2B′), suggesting that loss of *Foxc1* results in non-cell autonomous effects on *Msx2* expression. Similar changes in *Msx2* expression in *Foxc1* mutants were evident at E13.5 (Fig. 2E′,F′). These results suggest that Foxc1 acts to restrict the osteogenic domain and the *Msx2* expression domain within the supraorbital ridge. We note that *Msx2* expression does not expand into the innermost (endocranial) region of the *Foxc1* domain, suggesting that additional factors may be required for *Msx2* expression in this region.

To test directly whether Foxc1 negatively regulates *Msx2*, we used siRNA to knock down Foxc1 in cultured cells (Fig. 2H). In initial experiments, we used C3H10T1/2 cells, which are multipotent mesenchymal cells capable of differentiating into muscle cells, chondrocytes, adipocytes and osteoblasts (Pinney and Emerson, 1989; Katagiri et al., 1990). Because the mesenchyme of the supraorbital ridge at the level of the frontal bone rudiment is derived from cranial neural crest (Jiang et al., 2002; Ishii et al., 2003), we also used a cranial neural crest (CNC) cell line, O9-1, that we developed recently (Ishii et al., 2012). This cell line was derived from *Wnt1-Cre; R26R-EGFP*-expressing cells from the head region of E8.5 mouse embryos. We established culture conditions that allow O9-1 cells to be grown as multipotent stem-like cells, maintaining an ability to differentiate into osteoblasts, chondrocytes, smooth muscle cells and glial cells. O9-1 cells can be propagated and passaged indefinitely, and can contribute to bone and smooth muscle after injection into mouse embryos (Ishii et al., 2012). O9-1 cells undergo differentiation into osteoblasts with high efficiency after being placed into an osteogenic medium.

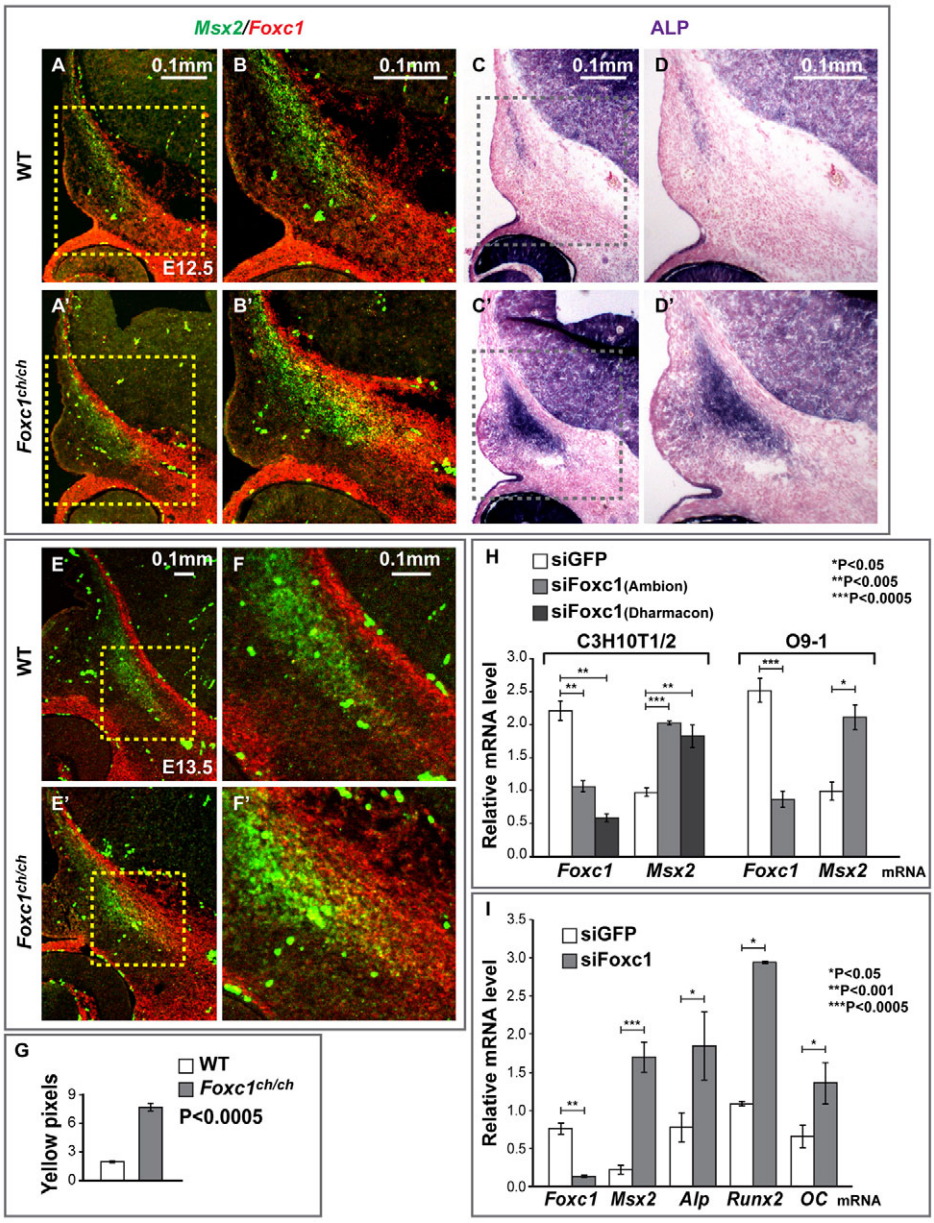

Fig. 2. Foxc1 inhibits *Msx2* expression in the supraorbital ridge and in cultured 10T1/2 and O9-1 cranial neural crest cells. (**A**,**A′**,**B**,**B′**,**E**,**E′**,**F**,**F′**) Control and *Foxc1*$^{ch/ch}$ embryos at E12.5 or E13.5 were sectioned as in Fig. 1A and subjected to *in situ* hybridization for *Msx2* and *Foxc1* mRNAs simultaneously. *Msx2* is in green; *Foxc1* in red. (**C-D′**) Sections from the same embryo were stained for ALP. Boxed areas are shown at higher magnification on the right. (**G**) The area of *Msx2* and *Foxc1* co-expression, indicated by the yellow color in B and B′, is significantly larger ($P<5.00\times10^{-4}$) in *Foxc1* mutants. (**H**) Effect of siRNA-mediated knockdown of Foxc1 on *Msx2* mRNA levels in C3H10T1/2 cells and O9-1 cranial neural crest cells. mRNA levels of *Foxc1* and *Msx2* were measured by qPCR and normalized to *Gapdh*. siRNA against EGFP provided a negative control. (**I**) We assessed the influence of Foxc1 knockdown on the rate of osteogenic differentiation of cultured O9-1 cells. Cells were treated with siRNA against Foxc1, and qPCR was used to measure levels of *Msx2*, ALP, *Runx2* and osteocalcin mRNAs. Significant ($P<0.05$) upregulation of each of these osteogenic differentiation markers was observed after 48 hours of Foxc1 siRNA treatment. Significance was assessed by Student's *t*-test. Error bars indicate s.d.

We transfected either a control siRNA or a Foxc1 siRNA into 10T1/2 and O9-1 cells, and assessed endogenous *Foxc1* and *Msx2* mRNA levels by real-time PCR (Fig. 2H). In 10T1/2 cells, *Foxc1* mRNA declined to 50% of its level in control cells, and *Msx2* transcript levels increased approximately twofold, consistent with Foxc1 exerting an inhibitory effect on *Msx2* expression. In O9-1 cells, Foxc1 siRNA caused a reduction of *Foxc1* mRNA to ~30% of its level in control siRNA-treated cells by 24 hours after transfection, and caused *Msx2* transcript levels to increase by approximately twofold. To rule out off-target effects, we used siRNAs against distinct sequences in the *Foxc1* transcript (Fig. 2H). These siRNAs (a mixture of four, none of which had sequences that overlapped with the siRNA used in the initial experiments) caused a similar reduction of *Foxc1* mRNA and increase in *Msx2* mRNA in both 10T1/2 (Fig. 2H) and O9-1 cells (data not shown). These results support the hypothesis that Foxc1 negatively regulates *Msx2* in the supraorbital ridge.

We next asked whether knockdown of Foxc1 augmented the osteogenic differentiation of O9-1 cells (Fig. 2I). We assessed the expression of the osteogenic markers *ALP*, *Runx2* and osteocalcin in Foxc1-knockdown and control O9-1 cells cultured in osteogenic medium. We found that the expression of each marker was increased relative to controls, suggesting that knockdown of Foxc1 not only upregulates *Msx2*, but also accelerates the osteogenic differentiation of O9-1 cells. These data support the hypothesis that reduced Foxc1 function can increase the rate of osteogenic differentiation of cranial neural crest cells.

Ectopic osteogenesis and *Msx2* expression correlate with ectopic Bmp signaling in calvarial rudiments of *Foxc1* mutants

We assessed the expression of *Bmp2*, *Bmp4*, P-Smad1/5/8 and the extracellular Bmp inhibitor *Noggin* in the calvarial rudiments and supraorbital ridge of *Foxc1*$^{ch/ch}$ mutant and control embryos (Fig. 3). We found that *Bmp2* and *Bmp4* expression domains were expanded at E12.5 and E13.5, similar to ALP (arrowheads, Fig. 3B′,C′,E′,G′; quantitation in 3M). In control embryos, *Noggin* transcripts were located ventral to the *Bmp*/ALP/*Msx2* domain (arrows, Fig. 3I,K). In

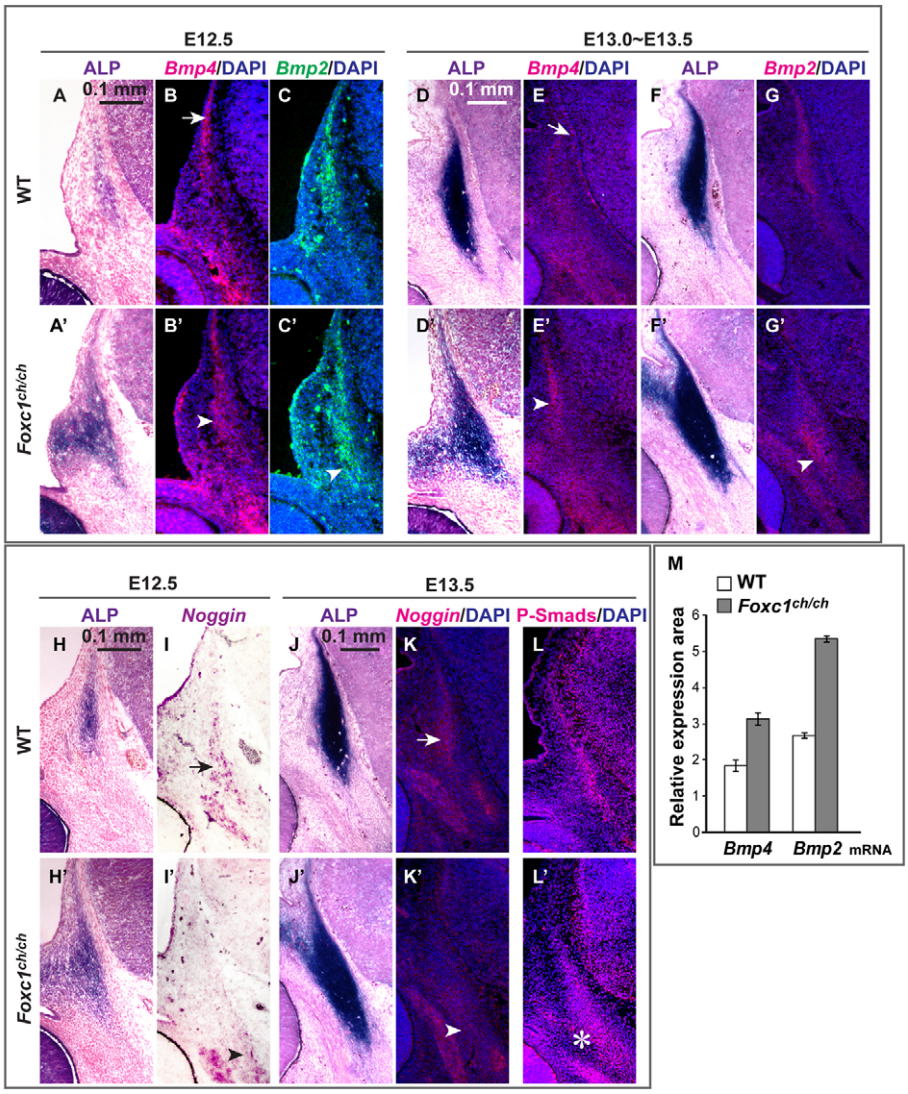

Fig. 3. Elevated Bmp signaling activity in the supraorbital ridge of *Foxc1* mutant embryos. (**A-G′**,**M**) We detected *Bmp4* and *Bmp2* expression by *in situ* hybridization in coronal sections of embryos at E12.5 and E13.5 wild-type and *Foxc1* mutant embryos. There is *Bmp4* expression at the apex of the osteogenic area and in the meninges of wild-type embryos (arrows, B and E), and in the rudiment of *Foxc1* mutants (arrowheads, B′ and E′). *Bmp2* expression is increased in the rudiment in *Foxc1* mutants (arrowheads, C′ and G′). The increases in both *Bmp4* and *Bmp2* expression in these areas were statistically significant at E12.5 (Student's *t*-test, $P<1.00\times10^{-8}$, M). Error bars indicate s.d. (**H-K′**) Expression of a Bmp antagonist, *Noggin*, assessed by *in situ* hybridization at E12.5 and E13.5. ALP was used to visualize the signal at E12.5 because it provided a more robust signal than fluorescent detection with extended developing time. *Noggin* transcripts are present in the rudiment and in an adjacent cartilage in wild-type embryos (arrows, I and K), but reduced in *Foxc1* mutants (arrowheads, I′ and K′). (**L**,**L′**) Immunodetection of P-Smad 1/5/8 served to indicate the overall activity of the canonical Bmp pathway. The number of P-Smad1/5/8-positive nuclei is increased in *Foxc1* mutant (asterisk, L′).

mutants, *Noggin* expression declined substantially (arrowheads, Fig. 3I′,K′). P-Smad1/5/8, the downstream effector of canonical Bmp signaling (Massagué, 1998), was distributed in a pattern that largely coincided with the *Bmp*/ALP/*Msx2* domain (Fig. 3L,L′). Expression expanded ventrally in the mutant (star, Fig. 3L′), consistent with a net increase in Bmp signaling in the area of ectopic ALP expression.

Reduced *Msx2* gene dose rescues ectopic osteogenesis and Bmp signaling in *Foxc1* mutants

To determine whether *Msx2* has a functional role downstream of *Foxc1* in the regulation of osteogenic precursor differentiation, we asked whether reduced *Msx2* dosage mitigated ectopic osteogenesis and Bmp signaling in *Foxc1* mutants (Fig. 4). We crossed *Msx2* and *Foxc1* mutants, producing embryos with the genotype $Foxc1^{ch/+}$; $Msx2^{+/-}$ and $Foxc1^{ch/ch}$; $Msx2^{+/-}$. We did not recover double homozygous null embryos from double heterozygous matings (n=59), consistent with this genotype causing lethality prior to E13. We assessed the size and growth of the calvarial rudiments by ALP staining of serial sections through the supraorbital ridge at E12.5 (Fig. 4A-F). $Foxc1^{ch/+}$ embryos exhibited a subtle but reproducible expansion of ALP, suggesting that this phenotype is *Foxc1* dose dependent at early developmental stages (supplementary material Fig. S1). However, this deficiency was transient, as frontal bone development was indistinguishable from wild type at E17 and P0 (Rice et al., 2003; J.S., M.I., M.-C.T. and R.M., unpublished).

The ectopic ALP staining evident in E12.5 $Foxc1^{ch/+}$ and $Foxc1^{ch/ch}$ mutant embryos was reduced or absent in *Foxc1/Msx2* double mutants (Fig. 4B-F). Quantitation of the ectopic ALP signal (e.g. Fig. 4H) by enumerating ALP pixels revealed reductions of 50% in both $Foxc1^{ch/+}$; $Msx2^{+/-}$ and $Foxc1^{ch/ch}$; $Msx2^{+/-}$ combinations. Similarly, ectopic P-Smad1/5/8 activity was reduced (Fig. 4J-N). These results suggest that the ectopic expression of *Msx2* resulting from loss of *Foxc1* function is causally related to ectopic osteogenesis and to Bmp signaling in the supraorbital ridge. Because $Foxc1^{ch/+}$ animals do not have a frontal bone phenotype at late stages of embryogenesis or in early postnatal life, we were unable to ask whether reduced *Msx2* dose rescued such animals. In addition, reduced *Msx2* dose did not rescue the hydrocephalus defect in $Foxc1^{ch/ch}$ embryos, precluding examination of such embryos at late stages.

Foxc1 acts through an upstream *Msx2* enhancer to regulate the *Msx2* expression domain and Bmp responsiveness in the supraorbital ridge

We next asked whether Foxc1 influences *Msx2* expression via an effect on an upstream *Msx2* enhancer (Fig. 5). ChIP experiments in

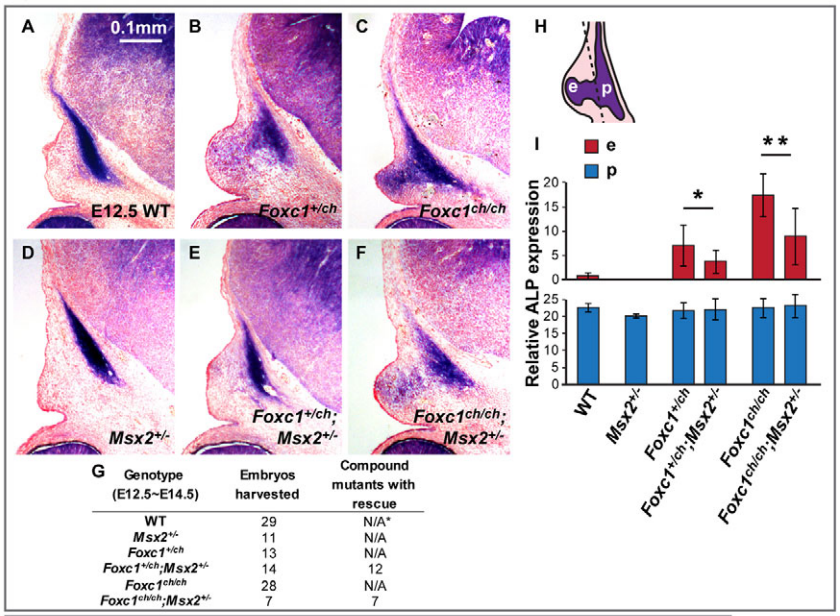

G Genotype (E12.5~E14.5)	Embryos harvested	Compound mutants with rescue
WT	29	N/A*
Msx2$^{+/-}$	11	N/A
Foxc1$^{+/ch}$	13	N/A
Foxc1$^{+/ch}$;*Msx2*$^{+/-}$	14	12
Foxc1$^{ch/ch}$	28	N/A
Foxc1$^{ch/ch}$;*Msx2*$^{+/-}$	7	7

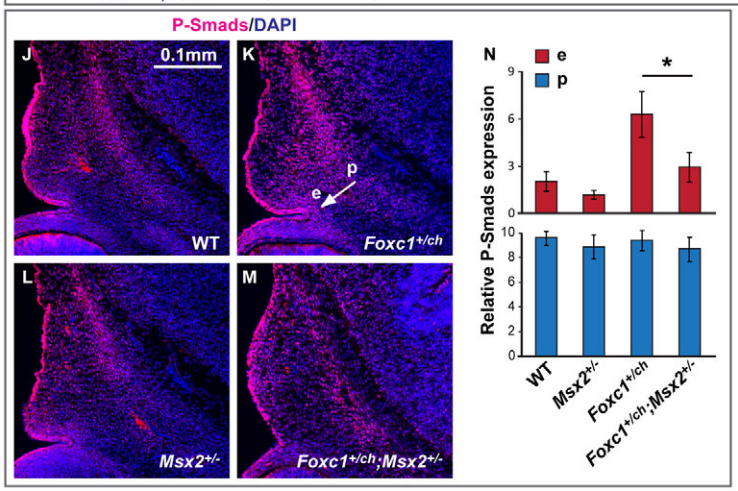

Fig. 4. Reduced dose of *Msx2* rescues ectopic osteogenesis and Bmp signaling in the supraorbital ridge of *Foxc1* mutant embryos. (**A-F**) ALP expression in the supraorbital ridge in E12.5 wild-type, *Foxc1*, *Msx2* and compound mutant embryos. There is near-normal expression of ALP in the *Foxc1*$^{ch/+}$;*Msx2*$^{+/-}$ compound heterozygous mutant (E) versus the *Foxc1* heterozygous mutant (B). Also note the partial rescue in the *Foxc1*$^{ch/ch}$;*Msx2*$^{+/-}$ mutant (F) compared with the *Foxc1* homozygous mutant (C). (**G**) Numbers of embryos harvested for this experiment. *N/A, not applicable. (**H**) We measured the level of ALP expression in the supraorbital ridge by counting the purple pixels in two areas: p (primordium) and e (ectopic). (**I**) The influence of *Msx2* dose on ALP expression in *Foxc1* mutants was statistically significant in area e (*P<0.05, **P<0.005). (**J-M**) Bmp signaling activity in E13 embryos was detected by P-Smad1/5/8 immunohistochemistry. P-Smad1/5/8 expansion is partially rescued: compare the area spanned by the white arrow from p to e in K with the corresponding area in M. (**N**) Significant reduction of P-Smad1/5/8 signal in area e in *Foxc1*$^{ch/+}$;*Msx2*$^{+/-}$ mutant embryo in comparison with *Foxc1*$^{ch/+}$ mutant (*P<5.00×10^{-6}). Significance was assessed by Student's *t*-test. Error bars indicate s.d.

ES cells and adult heart tissue showed that this enhancer is enriched for the transcription co-activator p300, as well as histone marks associated with active enhancers (Santos-Rosa et al., 2002; Bernstein et al., 2005; Chen et al., 2008; Visel et al., 2009) (Encode Project, UCSC Genome Browser).

We crossed mice carrying the *560bpMsx2-hsplacZ* transgene with *Foxc1* mutants (*Foxc1*$^{ch/+}$) and assessed its expression in the area of the frontal and parietal bone rudiments. *lacZ* expression expanded, similar to endogenous *Msx2* expression (Fig. 5D-E′). Therefore the 560 bp enhancer is sufficient to respond to a loss of *Foxc1* function.

Foxc1 negatively regulates *Msx2* expression and *Msx2* is an immediate early target of the Bmp signaling pathway (Brugger et al., 2004) suggesting that Foxc1 might inhibit the Bmp responsiveness of *Msx2*. To test this hypothesis, we implanted BMP2-soaked beads in the supraorbital ridge of explants of embryonic heads of E12.5 embryos (Fig. 5F). We cultured the explants and, after 2 days, carried out *in situ* hybridization with a probe for *Msx2* (Fig. 5G-H′). We found that the BMP2 beads elicited a greater increase in *Msx2* expression in *Foxc1* mutant embryos than in control embryos.

This result is in contrast to the findings of Rice et al. (Rice et al., 2003) who found that a BMP2-soaked bead implanted in the dorsum of the head of E15 embryos elicited a reduced Bmp response in *Foxc1* mutants compared with wild-type embryos. We repeated their experiment and obtained closely similar results; i.e. a reduction in Bmp responsiveness of *Msx2* (supplementary material Fig. S3). Therefore, the difference between our findings in the supraorbital ridge and those of Rice et al. (Rice et al., 2003) in the head mesenchyme is likely a consequence of the difference in the sites and developmental stages of bead implantation.

To further test the hypotheses that Foxc1 modulates the Bmp responsiveness of *Msx2*, and that the 560 bp enhancer is sufficient for this effect, we carried out a BMP2 bead implantation experiment in embryonic heads (Fig. 5I-J′) and limbs (data not shown) of mice carrying the *560bpMsx2-hsplacZ* transgene. Staining for β-galactosidase activity revealed that the 560 bp enhancer was indeed sufficient for the increase in the Bmp responsiveness of *Msx2* in *Foxc1* mutants in the supraorbital ridge.

Finally, we used both gain- and loss-of-function approaches in cultured cells to assess the influence of Foxc1 on the Bmp-responsiveness of *Msx2* (Fig. 5K-M). We transfected a construct bearing the 560 bp enhancer driving *tk-luciferase* (*560bpMsx2-tk-luc*) into 10T1/2 cells and O9-1 CNC cells, and tested the effect of overexpressing Foxc1 on the Bmp-inducibility of *560bpMsx2* (Fig. 5K,L). In both 10T1/2 and O9-1 cells, Bmp inducibility was more than halved (P<0.05). Reciprocally, transfection of siRNA

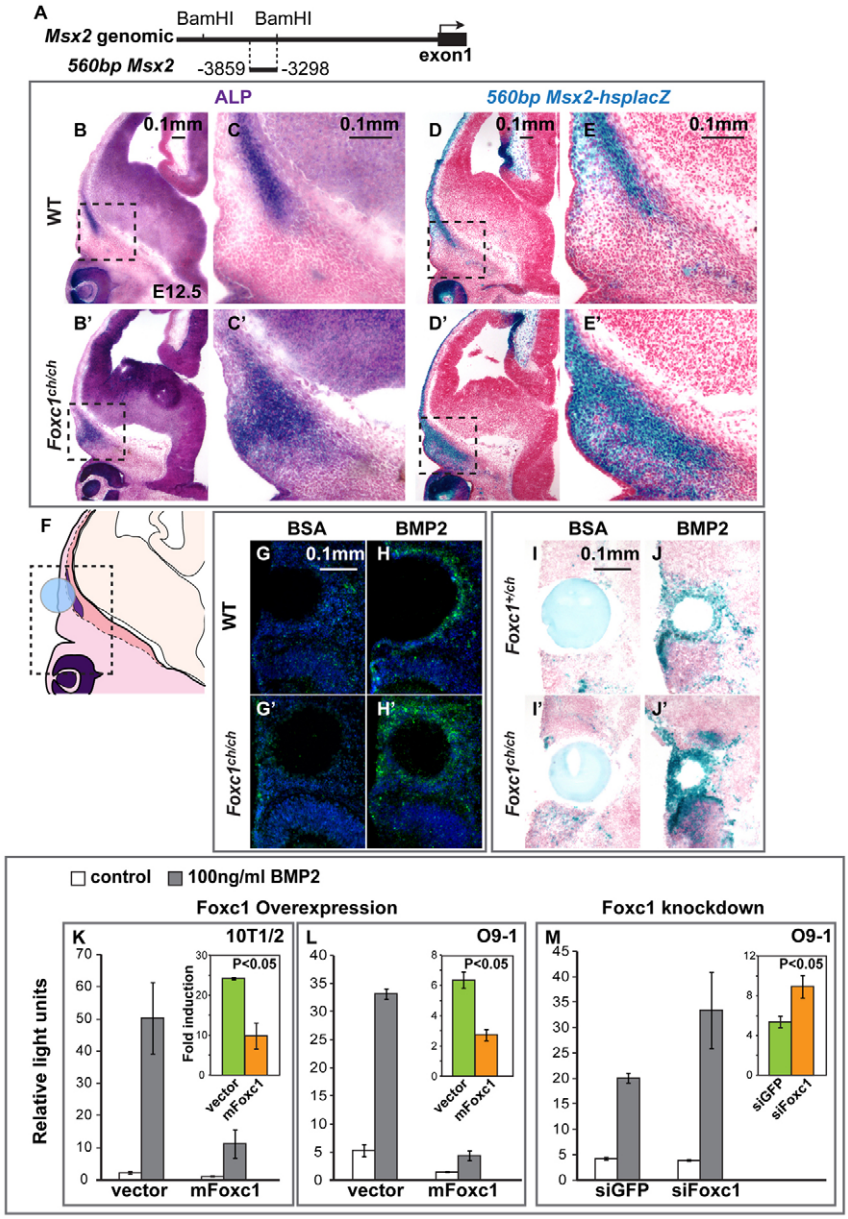

Fig. 5. Foxc1 inhibits the Bmp responsiveness of *Msx2* in embryos and cultured cells. (**A**) *Msx2* locus showing 560 bp *Msx2* upstream enhancer. (**B-E′**) ALP and *lacZ* staining was performed on adjacent sections of E12.5 *560bpMsx2-hsplacZ* transgenic embryos carrying either the wild-type (B-E) or *Foxc1*^{ch} mutant allele (B′-E′). Boxed areas are shown at higher magnification on the right. The *560bpMsx2* transgene is sufficient to respond to loss of *Foxc1* function. (**F-J′**) Influence of BMP2-soaked beads on endogenous *Msx2* (G-H′) assessed by *in situ* hybridization and *560bpMsx2-hsplacZ* expression (I-J′). The signal intensity in the supraorbital ridge is increased in both the endogenous *Msx2* (H versus H′) and the transgene (J versus J′) in *Foxc1* mutants compared with control embryos. (**K-M**) We tested the effect of overexpression (K,L) and siRNA-mediated knockdown (M) of Foxc1 on the Bmp inducibility of the *560bpMsx2-tk-luc* construct in 10T1/2 and O9-1 cranial neural crest cells. The insets show the fold change in luciferase expression. The results represent means of three biological replicates. Error bars show one s.d. Significance was assessed using Student's *t*-test.

against Foxc1 caused an increase in *560bpMsx2* Bmp inducibility in O9-1 cells of approximately twofold (P<0.05, Fig. 5M). These data support the hypothesis that Foxc1 regulates the Bmp responsiveness of *Msx2* through an effect on the 560 bp upstream enhancer.

Foxc1 is associated with the Bmp responsive element within the *Msx2* 560bp upstream enhancer

We next performed ChIP experiments to determine whether Foxc1 interacts with the endogenous *Msx2* locus in the area of the 560 bp enhancer when induced by BMP2 (Fig. 6). Using primers that flank the genomic region containing the 560 bp enhancer, and control primers against the β-actin promoter, we performed ChIP with a Foxc1 antibody on chromatin extracts derived from control or BMP2-treated O9-1 CNC and 10T1/2 cells (Fig. 6A). Treatment of both O9-1 cranial neural crest and 10T1/2 cells with BMP2 resulted in a substantial (approximately two- to threefold) enrichment of Foxc1 at the endogenous *Msx2* locus but not at the β-actin promoter (P<0.001). Quantitative RT-PCR showed that *Foxc1* mRNA is not increased upon treatment of O9-1 or 10T1/2 cells with BMP2 (Fig. 6B). The increase in Foxc1 at the *Msx2* enhancer is thus not controlled at the level of transcript accumulation.

To test whether Foxc1 interacts with the 52 bp Bmpre, we transfected into 10T1/2 cells a plasmid carrying only the 52 bp Bmpre driving *lacZ* (*52bpMsx2-hsplacZ*). ChIP assays with primers hybridizing with the plasmid sequence adjacent to the Bmpre (red arrows, Fig. 6C) showed that Foxc1 was enriched substantially at the Bmpre and that its occupancy at this site increased upon BMP2 treatment (P<0.005, Fig. 6D).

The AT-rich domain of the *Msx2* Bmpre has both an Antennapedia superclass recognition sequence (AATTAA) and an overlapping partial Fox site (AGCAATT, underlines) that matched the consensus (G/A)(T/C)(C/A)AA(T/C)A in 5/7 positions (Gao et al., 2003; Benayoun et al., 2011). To determine whether the interaction of Foxc1 with the Bmpre requires the AT-rich domain,

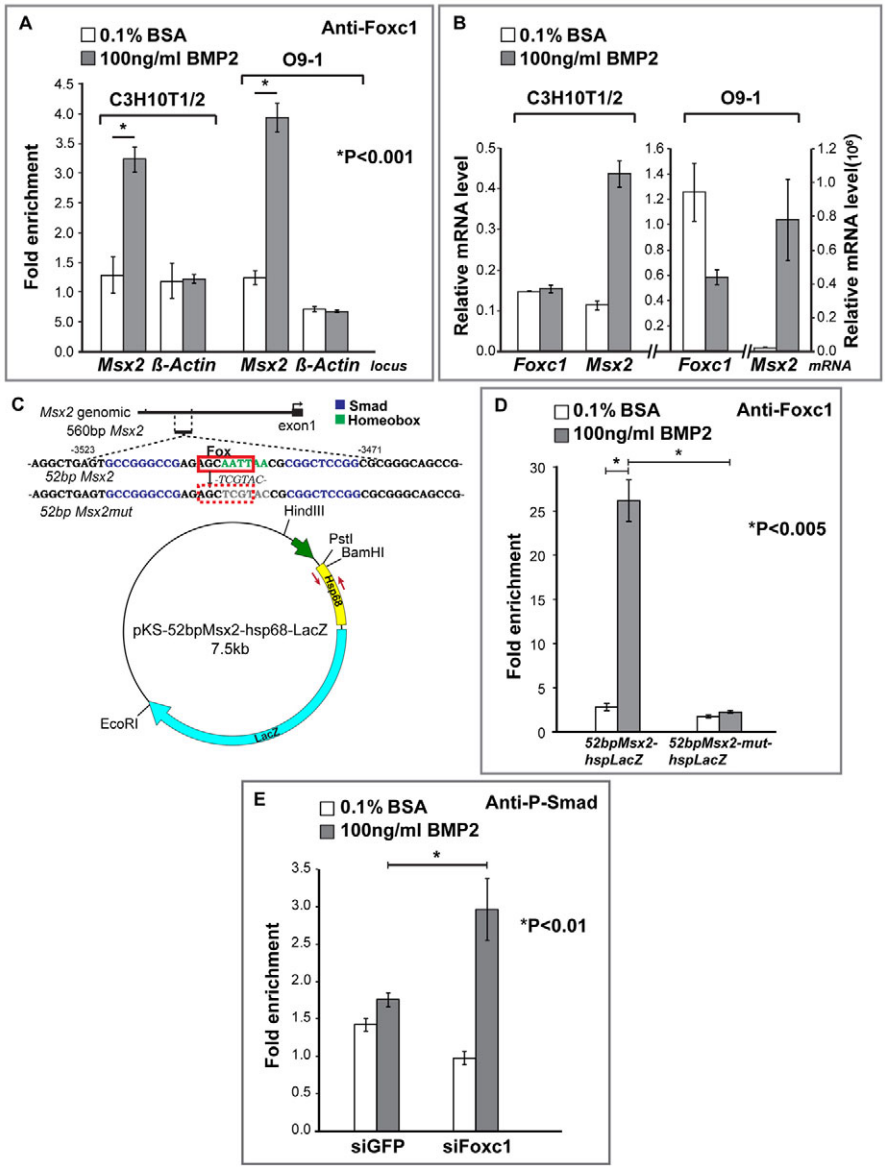

Fig. 6. Foxc1 interacts with a Bmp-responsive element in the 560 bp *Msx2* enhancer and inhibits the recruitment of P-Smad1/5/8. (**A**) Chromatin immunoprecipitation experiments in C3H10T1/2 and O9-1 cranial neural crest cells. We performed ChIP on control and BMP2-treated cells with an antibody against Foxc1 or rabbit IgG as a control. qPCR was used to amplify the 560 bp *Msx2* enhancer as well as a control β-actin promoter region. We show results of a single experiment (three PCR amplifications) representative of three independent experiments. Student's *t*-test was used to evaluate the strength of the difference between starred groups. Error bars represent one s.d. Foxc1 is enriched on the *Msx2* enhancer. (**B**) Effect of a 24-hour BMP2 treatment on *Foxc1* and *Msx2* mRNA level was evaluated by qPCR in both 10T1/2 and O9-1 cells. (**C**) The 52 bp *Msx2* Bmp-responsive element (Bmpre) (Brugger et al., 2004). Smad1 binding sites (blue) flank an AT-rich sequence (green). A partial Fox consensus binding site, AGCAATT [matching the consensus (G/A)(T/C)(C/A)AA(T/C)A in 5/7 positions (underlined)], overlapping the AT-rich sequence is boxed in red. (**D**) 10T1/2 cells were transfected with plasmids containing wild type (*52bpMsx2-hsplacZ*) or a mutant (*52bpMsx2-mut-hsplacZ*) in which the Fox site was mutated, and treated with BSA or BMP2 for 30 minutes. They were analyzed by ChIP with an anti-Foxc1 antibody or rabbit IgG as a control. qPCR was used to amplify a 200 bp *hsp68* fragment immediately downstream of the 52 bp *Msx2* (red arrows). We show results from at least three independent transfections. The interaction of Foxc1 with the Bmpre was almost completely abrogated by the mutation in the Fox/AT-rich element. (**E**) O9-1 cranial neural crest cells were treated with an siRNA against Foxc1 or EGFP. Cells were then treated with BSA or BMP2 and subjected to ChIP with an anti-P-Smad1 antibody or rabbit IgG. qPCR was used to amplify a 350 bp fragment in the 560 bp *Msx2* enhancer. Student's *t*-test was used to evaluate the strength of the difference between asterisked groups. Error bars represent one s.d.

we tested the effect of a mutation (*52bpMsx2-mut-hsplacZ*) in this domain on the association of Foxc1 with the 52 bp element. We transfected mutant and control constructs into 10T1/2 cells and asked whether we could detect Foxc1 by ChIP. As is evident in Fig. 6D, Foxc1 occupancy was reduced substantially relative to that of the control construct ($P<0.005$). Together, our findings support the view that Foxc1 acts directly on a Bmpre in the 560 bp enhancer upstream of *Msx2* to attenuate its Bmp responsiveness in the mesenchyme of the supraorbital ridge.

Foxc1 functions to exclude P-Smad1/5/8 from the *Msx2* Bmp responsive element

A simple mechanism that could explain the increased Bmp responsiveness of *Msx2* in *Foxc1* mutants is that Foxc1 attenuates the interaction of P-Smad1/5/8 with the *Msx2* Bmpre. Thus, loss of Foxc1 should result in an increase in P-Smad1/5/8 levels within the 560 bp enhancer. We used ChIP to assess P-Smad1/5/8 levels within the 560 bp enhancer in O9-1 cranial neural crest cells in which Foxc1 was knocked down by siRNA. Consistent with our hypothesis, we found that in Foxc1 knockdown cells, P-Smad1/5/8 levels were substantially higher than in control cells ($P<0.01$, Fig. 6E).

DISCUSSION

Here, we demonstrate a role for Foxc1 in regulating the influence of Bmp signaling on the expression of *Msx2* and the specification of osteogenic precursor cells in the developing skull vault. Using both mouse embryos and a cranial neural crest cell line, we show that Foxc1 acts directly on a Bmp-responsive enhancer to reduce the occupancy of P-Smad1/5/8 and thus restrict *Msx2* expression to an osteogenic zone fated to become the developing frontal bone. We propose that within the supraorbital ridge, Foxc1 functions through *Msx2* to set a threshold level of Bmp signaling activity, thus controlling the differentiation of osteogenic precursor cells and the development of the calvarial bones.

Rice and colleagues first suggested a relationship between *Foxc1* and *Msx2* (Rice et al., 2003). These authors showed that BMP2 beads implanted in the head mesenchyme of E15 *Foxc1* mutants stimulated expression of *Msx2* to a lesser extent than in wild-type mice, leading to the conclusion that Bmp-induced expression of

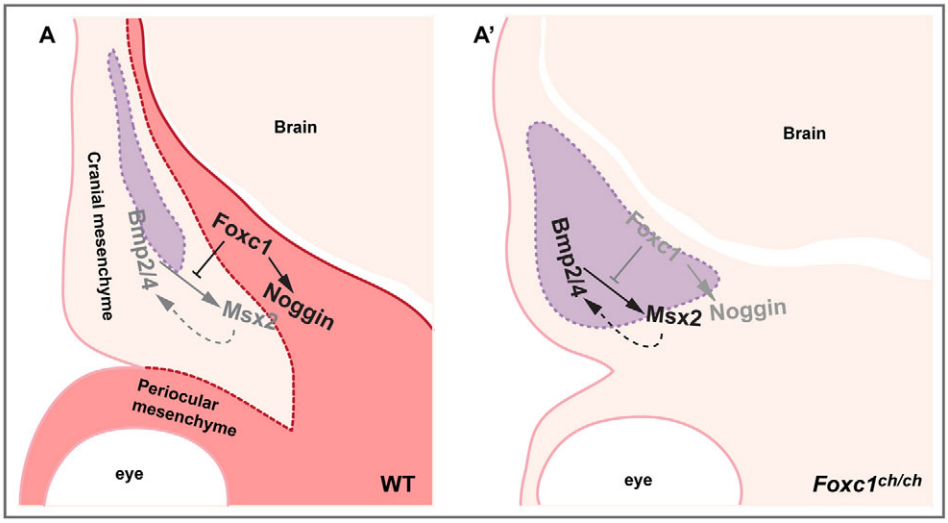

Fig. 7. Schematic model showing role of Foxc1 regulating Bmp signaling and osteoprogenitor development in the supraorbital ridge. *Foxc1* is expressed in the meninges and adjacent mesenchyme (red in A). Osteogenic cells are marked with purple shading. (**A**) In wild-type embryos, Foxc1 negatively regulates *Msx2* and *Bmp2/4*, and positively regulates *Noggin*, thereby maintaining levels of Bmp signaling appropriate for the migration of progenitor cells into the frontal bone rudiment and their differentiation into osteoblasts. (**A′**) In *Foxc1* mutants, loss of *Foxc1* results in upregulation of *Msx2*, which initiates a positive-feedback loop between *Msx2* and *Bmp2/4*. The result is the propagation of a wave of *Msx2* and *Bmp2/4* expression from medial to lateral across the supraorbital ridge, and the lateral displacement of the boundary between ALP-expressing cells of the frontal bone rudiment and adjacent non-ALP expressing mesenchyme.

Msx2 requires *Foxc1*. We were thus surprised at first by our finding that Foxc1 negatively regulates *Msx2*. We note, however, that Rice et al. (Rice et al., 2003) implanted Bmp beads in the dorsum of the head of E15 embryos, whereas we implanted them in the supraorbital ridge of E12.5 embryos. We repeated the bead implantation performed by Rice et al. (Rice et al., 2003) and obtained similar results (supplementary material Fig. S3). Thus, our finding of increased *Msx2* expression and Bmp responsiveness in the supraorbital ridge of *Foxc1* mutants is not in conflict with the findings of Rice et al. (Rice et al., 2003), but instead is likely a result of the different site or developmental stage of bead implantation. While this work was under review, Mirzayans and colleagues, working in several mouse and human cell lines, reported that FOXC1 positively regulates *Msx2* (Mirzayans et al., 2012). They identified a 480 bp proximal promoter fragment that contains a FOXC1-binding site and is sufficient to respond to FOXC1. This fragment is distinct from the 560 bp *Msx2* enhancer. These findings underline our conclusion that the nature of the interaction between *Foxc1* and *Msx2* is highly dependent on cellular context. The molecular details of how Foxc1 represses *Msx2* gene activity in one context and activates it in another remain obscure, but are likely to reflect the ability of Foxc1 to recruit either co-activators or co-repressors to target promoters. It is thus interesting that in zebrafish podocytes, Foxc1a can both activate and repress the *Podocalyxin* promoter, depending on the dose of Foxc1 relative to an interacting transcription factor, Wt1 (O'Brien et al., 2011).

The supraorbital ridge domain is crucial for the development of the skull vault. DiI labeling and recent Cre-based lineage-tracing experiments (Yoshida et al., 2008; Ting et al., 2009; Roybal et al., 2010; Deckelbaum et al., 2012) show that at E11.5 undifferentiated precursor cells of the frontal and parietal bones, as well as the coronal suture, are located in the supraorbital ridge. These cells subsequently migrate apically and contribute to the growing bones and suture. These cells are defined functionally by their ability to contribute to the ALP-positive frontal and parietal bone rudiments and the ALP-negative coronal suture between them. Our data show that the distribution of neural crest and mesoderm within the supraorbital ridge is not grossly changed in *Foxc1* mutants compared with controls. Given this, our finding that the frontal bone rudiment begins to develop in *Foxc1* mutants but does not elongate suggests that the deficiency in *Foxc1* mutants is not in the migration of the precursors into the supraorbital ridge, but in their development during the apical growth phase of calvarial development. The expansion of ALP across the ridge strongly suggests a mechanism that could slow or prevent elongation – the depletion of precursors by differentiation. That knockdown of Foxc1 in cultured neural crest cells accelerates the differentiation of such cells also supports this model. We note that Rice and colleagues documented a reduction in proliferation of cells within the rudiments of *Foxc1* mutants (Rice et al., 2003). Such a reduction could also contribute to the slowed calvarial growth. We point out, finally, that as *Foxc1* homozygous mutants do not survive into late embryogenesis and heterozygotes do not have a skull phenotype, we do not yet know the consequences of the premature differentiation of osteogenic precursor cells in supraorbital ridge on the later development of skull vault. Addressing this issue will have to await the conditional inactivation of *Foxc1* in prospective calvarial tissues, an approach made possible by the recent generation of a conditional *Foxc1* mutant allele (Sasman et al., 2012).

It is well established that Bmp signaling controls the differentiation of osteogenic precursor cells in the frontal and parietal bone rudiments (Kim et al., 1998). There is also evidence that reduced dose of *Msx1/2* results in reduced numbers of osteogenic precursor cells in calvarial bone rudiments, and reduced calvarial bone growth (Ishii et al., 2003; Han et al., 2007). Given that Msx genes are known to be transcriptional effectors of Bmp signaling (Vainio et al., 1993; Graham et al., 1994; Bei and Maas,

1998), our finding that Foxc1 negatively regulates the Bmp inducibility of *Msx2* in the mesenchyme of the supraorbital ridge and in cultured cranial neural crest cells suggests that Foxc1 controls a Bmp threshold response of *Msx2*. Reduced Foxc1 activity lowers the threshold (i.e. makes *Msx2* more sensitive to Bmp induction); increased Foxc1 activity raises it. This threshold, we propose, regulates the balance between the maintenance of an undifferentiated precursor cell population on the one hand, and the differentiation of osteogenic precursors as they move into the high Bmp environment of the frontal bone rudiment, on the other.

Our data suggest that the expression domain of *Foxc1* has only a narrow region of overlap with that of *Msx2*, yet the influence of Foxc1 on *Msx2* expression spans a much wider area. The overlapping region includes parts of the dura and the mesenchyme immediately adjacent to the dura. We were surprised to find that in *Foxc1* mutants, *Msx2* is upregulated over the major part of the supraorbital ridge, not just in the *Foxc1-Msx2* overlapping region. ALP, *Bmp2* and *Bmp4* expand similarly across this region. Thus, loss of *Foxc1* results in a non-autonomous cascade of changes in gene expression across the supraorbital ridge. We propose that the expansion of *Msx2*, as well as that of ALP, *Bmp2* and *Bmp4*, is the result of a positive-feedback loop between Bmp signaling and *Msx2*: in the absence of *Foxc1*, *Msx2* is upregulated in the *Foxc1* domain, resulting in upregulation of Bmp genes in this same domain. Bmp proteins are able to signal adjacent cells, resulting in upregulation of *Msx2*, and in turn a further expansion of Bmp gene expression. The net result is a wave of *Msx2* and *Bmp* expression that spreads from medial to lateral across the supraorbital ridge. This, we suggest, results in the ectopic differentiation of supraorbital mesenchyme to ALP-positive osteogenic cells.

Direct functional evidence for a *Foxc1-Msx2-Bmp* loop comes from the genetic reduction of *Msx2* activity in the *Foxc1* mutant. This results not only in a rescue of *Msx2* expression, but also of P-Smad1/5/8 activity. Thus, our results show that *Msx2* is required downstream of *Foxc1* to maintain cells of the supraorbital ridge in an undifferentiated state. It is intriguing that loss of *Foxc1* also results in reduced *Noggin* expression and increased P-Smad1/5/8 activity in a localized area medial to the growing rudiment. We do not know that fate of these *Noggin*-expressing cells, but speculate that they may be osteogenic precursors. DiI labeling experiments show such precursor cells are present in the supraorbital ridge (Yoshida et al., 2008; Ting et al., 2009).

The *Foxc1-Msx2-Bmp* regulatory loop has some features of a bistable system (Ferrell, 2002). Such systems contain positive or double-negative feedback loops whose component genes typically respond to their upstream regulators in an ultrasensitive manner (Furtado et al., 2008). Bistable systems function to convert graded inputs into switch-like responses (Ferrell, 2002). In the case of the *Foxc1/Msx2/Bmp* axis, we propose that a positive loop between *Bmp* and *Msx2* is modulated by negative regulation of *Msx2* by Foxc1. The net result of this Foxc1-dependent regulation of the *Msx2-Bmp* loop is a sharp boundary between differentiating osteogenic cells of the rudiments and undifferentiated cells of the mesenchyme lateral to the rudiments (Fig. 7). An apparently graded Bmp input is thus converted into a sharp functional boundary. Loss of *Foxc1* function results in a blurring of the boundary.

Experiments in cultured CNC cells and 10T1/2 cells support the view that Foxc1 can act directly on *Msx2*. These experiments show: (1) that Foxc1 is associated with chromatin in the area of a 52 bp Bmp-responsive element within an upstream *Msx2* enhancer; and (2) that the Foxc1 interaction is abrogated by a mutation that targets both a Foxc1 consensus site and an overlapping AATTAA site. Moreover, loss of Foxc1 results in increased Bmp-inducibility of endogenous *Msx2*. That we obtained similar results in 10T1/2 cells and in the O9-1 cranial neural crest cell line strengthens the argument for a direct, negative regulatory interaction between *Foxc1* and *Msx2*.

Our data suggest a molecular mechanism by which reduced Foxc1 activity could influence *Msx2* transcription. We have found that loss of *Foxc1* function in cranial neural crest and 10T1/2 cells results in an increase in P-Smad1/5/8 in the region of the 560 bp enhancer. Given the crucial function of P-Smad1/5/8 in Bmp-dependent transcription (Massagué, 1998; Massagué, 2000), this increase could explain the enhanced Bmp inducibility of *Msx2* when Foxc1 activity is reduced genetically or by siRNA. How this reciprocal relationship between Foxc1 and P-Smad1/5/8 enhancer occupancy might work on a molecular level is not yet clear. Foxc1 and Smad1 are not known to interact. However, FoxO proteins can interact with Smad4 to modulate Tgfβ signaling (Seoane et al., 2004; Gomis et al., 2006). Moreover, Foxc1 can associate with Smad4, which is also required for Bmp-dependent signaling and is found in a transcriptional complex with Smad1 (Lagna et al., 1996; Kretzschmar et al., 1997). Thus, loss of Foxc1 could act through Smad4 to affect indirectly the ability of Smad1 to participate in a complex on the enhancer.

Acknowledgements

J.S. thanks Dr Mamoru Ishii for the hypothesis that led to her fellowship from the California Institute of Regenerative Medicine. We also thank Dr Deborah Johnson for advice on siRNA and members of Dr Michael Stallcup's laboratory for help with ChIP and qPCR analyses.

Funding

This work was supported by grants from the National Institutes of Health [R01DE016320 and R01DE019650 to R.M.]. J.S. was supported by a fellowship from the California Institute of Regenerative Medicine [T100004]. Deposited in PMC for release after 12 months.

Competing interests statement

The authors declare no competing financial interests.

Supplementary material

Supplementary material available online at
http://dev.biologists.org/lookup/suppl/doi:10.1242/dev.085225/-/DC1

References

Aldinger, K. A., Lehmann, O. J., Hudgins, L., Chizhikov, V. V., Bassuk, A. G., Ades, L. C., Krantz, I. D., Dobyns, W. B. and Millen, K. J. (2009). FOXC1 is required for normal cerebellar development and is a major contributor to chromosome 6p25.3 Dandy-Walker malformation. *Nat. Genet.* **41**, 1037-1042.

Bach, A., Lallemand, Y., Nicola, M. A., Ramos, C., Mathis, L., Maufras, M. and Robert, B. (2003). Msx1 is required for dorsal diencephalon patterning. *Development* **130**, 4025-4036.

Bei, M. and Maas, R. (1998). FGFs and BMP4 induce both Msx1-independent and Msx1-dependent signaling pathways in early tooth development. *Development* **125**, 4325-4333.

Benayoun, B. A., Caburet, S. and Veitia, R. A. (2011). Forkhead transcription factors: key players in health and disease. *Trends Genet.* **27**, 224-232.

Bernstein, B. E., Kamal, M., Lindblad-Toh, K., Bekiranov, S., Bailey, D. K., Huebert, D. J., McMahon, S., Karlsson, E. K., Kulbokas, E. J., 3rd, Gingeras, T. R. et al. (2005). Genomic maps and comparative analysis of histone modifications in human and mouse. *Cell* **120**, 169-181.

Brugger, S. M., Merrill, A. E., Torres-Vazquez, J., Wu, N., Ting, M. C., Cho, J. Y., Dobias, S. L., Yi, S. E., Lyons, K., Bell, J. R. et al. (2004). A phylogenetically conserved cis-regulatory module in the Msx2 promoter is sufficient for BMP-dependent transcription in murine and Drosophila embryos. *Development* **131**, 5153-5165.

Chai, Y. and Maxson, R. E., Jr (2006). Recent advances in craniofacial morphogenesis. *Dev. Dyn.* **235**, 2353-2375.

Chen, Y. H., Ishii, M., Sun, J., Sucov, H. M. and Maxson, R. E., Jr (2007). Msx1 and Msx2 regulate survival of secondary heart field precursors and post-migratory proliferation of cardiac neural crest in the outflow tract. *Dev. Biol.* **308**, 421-437.

Chen, X., Xu, H., Yuan, P., Fang, F., Huss, M., Vega, V. B., Wong, E., Orlov, Y. L., Zhang, W., Jiang, J. et al. (2008). Integration of external signaling pathways with the core transcriptional network in embryonic stem cells. *Cell* **133**, 1106-1117.
Deckelbaum, R. A., Holmes, G., Zhao, Z., Tong, C., Basilico, C. and Loomis, C. A. (2012). Regulation of cranial morphogenesis and cell fate at the neural crest-mesoderm boundary by engrailed 1. *Development* **139**, 1346-1358.
Ferrell, J. E., Jr (2002). Self-perpetuating states in signal transduction: positive feedback, double-negative feedback and bistability. *Curr. Opin. Cell Biol.* **14**, 140-148.
Furtado, M. B., Solloway, M. J., Jones, V. J., Costa, M. W., Biben, C., Wolstein, O., Preis, J. I., Sparrow, D. B., Saga, Y., Dunwoodie, S. L. et al. (2008). BMP/SMAD1 signaling sets a threshold for the left/right pathway in lateral plate mesoderm and limits availability of SMAD4. *Genes Dev.* **22**, 3037-3049.
Gao, N., Zhang, J., Rao, M. A., Case, T. C., Mirosevich, J., Wang, Y., Jin, R., Gupta, A., Rennie, P. S. and Matusik, R. J. (2003). The role of hepatocyte nuclear factor-3 alpha (Forkhead Box A1) and androgen receptor in transcriptional regulation of prostatic genes. *Mol. Endocrinol.* **17**, 1484-1507.
Gomis, R. R., Alarcón, C., He, W., Wang, Q., Seoane, J., Lash, A. and Massagué, J. (2006). A FoxO-Smad synexpression group in human keratinocytes. *Proc. Natl. Acad. Sci. USA* **103**, 12747-12752.
Graham, A., Francis-West, P., Brickell, P. and Lumsden, A. (1994). The signalling molecule BMP4 mediates apoptosis in the rhombencephalic neural crest. *Nature* **372**, 684-686.
Gurdon, J. B. and Bourillot, P. Y. (2001). Morphogen gradient interpretation. *Nature* **413**, 797-803.
Gurdon, J. B., Mitchell, A. and Mahony, D. (1995). Direct and continuous assessment by cells of their position in a morphogen gradient. *Nature* **376**, 520-521.
Han, J., Ishii, M., Bringas, P., Jr, Maas, R. L., Maxson, R. E., Jr and Chai, Y. (2007). Concerted action of Msx1 and Msx2 in regulating cranial neural crest cell differentiation during frontal bone development. *Mech. Dev.* **124**, 729-745.
Hannenhalli, S. and Kaestner, K. H. (2009). The evolution of Fox genes and their role in development and disease. *Nat. Rev. Genet.* **10**, 233-240.
Ishii, M., Merrill, A. E., Chan, Y. S., Gitelman, I., Rice, D. P., Sucov, H. M. and Maxson, R. E., Jr (2003). Msx2 and Twist cooperatively control the development of the neural crest-derived skeletogenic mesenchyme of the murine skull vault. *Development* **130**, 6131-6142.
Ishii, M., Arias, A. C., Liu, L., Chen, Y. B., Bronner, M. E. and Maxson, R. E. (2012). A stable cranial neural crest cell line from mouse. *Stem Cells Dev.* **21**, 3069-3080.
Jiang, X., Iseki, S., Maxson, R. E., Sucov, H. M. and Morriss-Kay, G. M. (2002). Tissue origins and interactions in the mammalian skull vault. *Dev. Biol.* **241**, 106-116.
Katagiri, T., Yamaguchi, A., Ikeda, T., Yoshiki, S., Wozney, J. M., Rosen, V., Wang, E. A., Tanaka, H., Omura, S. and Suda, T. (1990). The non-osteogenic mouse pluripotent cell line, C3H10T1/2, is induced to differentiate into osteoblastic cells by recombinant human bone morphogenetic protein-2. *Biochem. Biophys. Res. Commun.* **172**, 295-299.
Kim, H. J., Rice, D. P., Kettunen, P. J. and Thesleff, I. (1998). FGF-, BMP- and Shh-mediated signalling pathways in the regulation of cranial suture morphogenesis and calvarial bone development. *Development* **125**, 1241-1251.
Kretzschmar, M., Liu, F., Hata, A., Doody, J. and Massagué, J. (1997). The TGF-beta family mediator Smad1 is phosphorylated directly and activated functionally by the BMP receptor kinase. *Genes Dev.* **11**, 984-995.
Kume, T., Deng, K. Y., Winfrey, V., Gould, D. B., Walter, M. A. and Hogan, B. L. (1998). The forkhead/winged helix gene Mf1 is disrupted in the pleiotropic mouse mutation congenital hydrocephalus. *Cell* **93**, 985-996.
Kume, T., Deng, K. and Hogan, B. L. (2000). Murine forkhead/winged helix genes Foxc1 (Mf1) and Foxc2 (Mfh1) are required for the early organogenesis of the kidney and urinary tract. *Development* **127**, 1387-1395.
Kume, T., Jiang, H., Topczewska, J. M. and Hogan, B. L. (2001). The murine winged helix transcription factors, Foxc1 and Foxc2, are both required for cardiovascular development and somitogenesis. *Genes Dev.* **15**, 2470-2482.
Kwang, S. J., Brugger, S. M., Lazik, A., Merrill, A. E., Wu, L. Y., Liu, Y. H., Ishii, M., Sangiorgi, F. O., Rauchman, M., Sucov, H. M. et al. (2002). Msx2 is an immediate downstream effector of Pax3 in the development of the murine cardiac neural crest. *Development* **129**, 527-538.
Lagna, G., Hata, A., Hemmati-Brivanlou, A. and Massagué, J. (1996). Partnership between DPC4 and SMAD proteins in TGF-beta signalling pathways. *Nature* **383**, 832-836.
Ma, H., Shang, Y., Lee, D. Y. and Stallcup, M. R. (2003). Study of nuclear receptor-induced transcription complex assembly and histone modification by chromatin immunoprecipitation assays. *Methods Enzymol.* **364**, 284-296.
Massagué, J. (1998). TGF-beta signal transduction. *Annu. Rev. Biochem.* **67**, 753-791.
Massagué, J. (2000). How cells read TGF-beta signals. *Nat. Rev. Mol. Cell Biol.* **1**, 169-178.
Mirzayans, F., Lavy, R., Penner-Chea, J. and Berry, F. B. (2012). Initiation of early osteoblast differentiation events through the direct transcriptional regulation of Msx2 by FOXC1. *PLoS ONE* **7**, e49095.
Morriss-Kay, G. M. and Wilkie, A. O. (2005). Growth of the normal skull vault and its alteration in craniosynostosis: insights from human genetics and experimental studies. *J. Anat.* **207**, 637-653.
O'Brien, L. L., Grimaldi, M., Kostun, Z., Wingert, R. A., Selleck, R. and Davidson, A. J. (2011). Wt1a, Foxc1a, and the Notch mediator Rbpj physically interact and regulate the formation of podocytes in zebrafish. *Dev. Biol.* **358**, 318-330.
Paratore, C., Suter, U. and Sommer, L. (1999). Embryonic gene expression resolved at the cellular level by fluorescence in situ hybridization. *Histochem. Cell Biol.* **111**, 435-443.
Phippard, D. J., Weber-Hall, S. J., Sharpe, P. T., Naylor, M. S., Jayatalake, H., Maas, R., Woo, I., Roberts-Clark, D., Francis-West, P. H., Liu, Y. H. et al. (1996). Regulation of Msx-1, Msx-2, Bmp-2 and Bmp-4 during foetal and postnatal mammary gland development. *Development* **122**, 2729-2737.
Pinney, D. F. and Emerson, C. P., Jr (1989). 10T1/2 cells: an in vitro model for molecular genetic analysis of mesodermal determination and differentiation. *Environ. Health Perspect.* **80**, 221-227.
Rice, R., Rice, D. P., Olsen, B. R. and Thesleff, I. (2003). Progression of calvarial bone development requires Foxc1 regulation of Msx2 and Alx4. *Dev. Biol.* **262**, 75-87.
Roybal, P. G., Wu, N. L., Sun, J., Ting, M. C., Schafer, C. A. and Maxson, R. E. (2010). Inactivation of Msx1 and Msx2 in neural crest reveals an unexpected role in suppressing heterotopic bone formation in the head. *Dev. Biol.* **343**, 28-39.
Santos-Rosa, H., Schneider, R., Bannister, A. J., Sherriff, J., Bernstein, B. E., Emre, N. C., Schreiber, S. L., Mellor, J. and Kouzarides, T. (2002). Active genes are tri-methylated at K4 of histone H3. *Nature* **419**, 407-411.
Sasman, A., Nassano-Miller, C., Shim, K. S., Koo, H. Y., Liu, T., Schultz, K. M., Millay, M., Nanano, A., Kang, M., Suzuki, T. et al. (2012). Generation of conditional alleles for Foxc1 and Foxc2 in mice. *Genesis* **50**, 766-774.
Satokata, I. and Maas, R. (1994). Msx1 deficient mice exhibit cleft palate and abnormalities of craniofacial and tooth development. *Nat. Genet.* **6**, 348-356.
Satokata, I., Ma, L., Ohshima, H., Bei, M., Woo, I., Nishizawa, K., Maeda, T., Takano, Y., Uchiyama, M., Heaney, S. et al. (2000). Msx2 deficiency in mice causes pleiotropic defects in bone growth and ectodermal organ formation. *Nat. Genet.* **24**, 391-395.
Seo, S. and Kume, T. (2006). Forkhead transcription factors, Foxc1 and Foxc2, are required for the morphogenesis of the cardiac outflow tract. *Dev. Biol.* **296**, 421-436.
Seoane, J., Le, H. V., Shen, L., Anderson, S. A. and Massagué, J. (2004). Integration of Smad and forkhead pathways in the control of neuroepithelial and glioblastoma cell proliferation. *Cell* **117**, 211-223.
Ting, M. C., Wu, N. L., Roybal, P. G., Sun, J., Liu, L., Yen, Y. and Maxson, R. E., Jr (2009). EphA4 as an effector of Twist1 in the guidance of osteogenic precursor cells during calvarial bone growth and in craniosynostosis. *Development* **136**, 855-864.
Tümer, Z. and Bach-Holm, D. (2009). Axenfeld-Rieger syndrome and spectrum of PITX2 and FOXC1 mutations. *Eur. J. Hum. Genet.* **17**, 1527-1539.
Vainio, S., Karavanova, I., Jowett, A. and Thesleff, I. (1993). Identification of BMP-4 as a signal mediating secondary induction between epithelial and mesenchymal tissues during early tooth development. *Cell* **75**, 45-58.
Visel, A., Blow, M. J., Li, Z., Zhang, T., Akiyama, J. A., Holt, A., Plajzer-Frick, I., Shoukry, M., Wright, C., Chen, F. et al. (2009). ChIP-seq accurately predicts tissue-specific activity of enhancers. *Nature* **457**, 854-858.
Wilkie, A. O., Tang, Z., Elanko, N., Walsh, S., Twigg, S. R., Hurst, J. A., Wall, S. A., Chrzanowska, K. H. and Maxson, R. E., Jr (2000). Functional haploinsufficiency of the human homeobox gene MSX2 causes defects in skull ossification. *Nat. Genet.* **24**, 387-390.
Yoshida, T., Vivatbutsiri, P., Morriss-Kay, G., Saga, Y. and Iseki, S. (2008). Cell lineage in mammalian craniofacial mesenchyme. *Mech. Dev.* **125**, 797-808.
Zarbalis, K., Siegenthaler, J. A., Choe, Y., May, S. R., Peterson, A. S. and Pleasure, S. J. (2007). Cortical dysplasia and skull defects in mice with a Foxc1 allele reveal the role of meningeal differentiation in regulating cortical development. *Proc. Natl. Acad. Sci. USA* **104**, 14002-14007.